Behavior of Prestressed Concrete Box-Beam Bridges Using CFRP Tendons

Nabil F. Grace
Professor and Chair
Civil Engineering Department
Director, Center for Innovative Materials Research
Lawrence Technological University
Southfield, Mich.

Shamsher B. Singh
Research Engineer
Civil Engineering Department
Lawrence Technological University
Southfield, Mich.

Sreejith Puravankara
Graduate Student
Civil Engineering Department
Lawrence Technological University
Southfield, Mich.

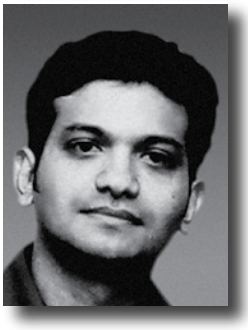

Saju Sachidanandan
Graduate Student
Civil Engineering Department
Lawrence Technological University
Southfield, Mich.

This paper presents the results of an experimental and analytical study of the flexural response of concrete box beams prestressed with carbon fiber reinforced polymer (CFRP) tendons Diversified Composites Inc. (DCI) for three highway bridge models. Each bridge model comprises two precast concrete box beams pretensioned using DCI tendons. In one of the bridge models, the box beams were also prestressed using 12 unbonded, DCI post-tensioning tendons. In the second bridge model, the box beams were not provided with post-tensioning tendons. The third bridge model comprised box beams provided with 12 unbonded tendons without any force. This study consisted of predicting parameters such as transfer lengths of DCI tendons, ultimate loads, deflections, post-tensioning forces, strains, and energy ratios. This paper also presents a comparison of experimental and analytical results. It was observed that the measured transfer lengths of DCI tendons ranged from 25 to 32 times the nominal tendon diameter. The bridge model comprising box beams prestressed using both pretensioning and unbonded post-tensioning tendons resulted in higher load capacity and lower ductility compared with the other two bridge models. The close agreement between experimental and analytical values signifies the accuracy of a strain-controlled approach in analyzing CFRP box-beam bridge models.

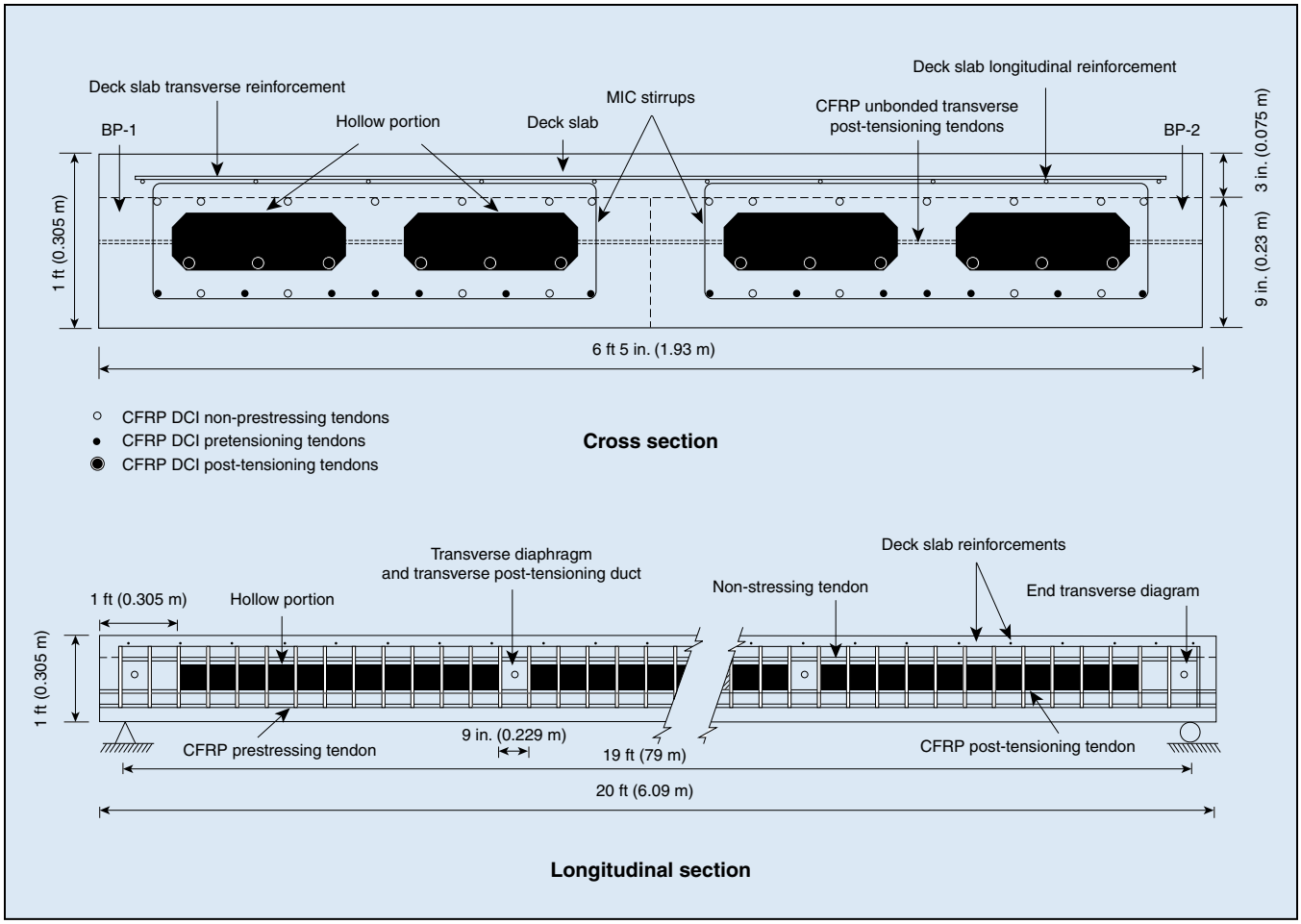

Fig. 1. Cross-section details and longitudinal section of BBD-I. Note: 1 ft = 0.305 m; 1 in. = 25.4 mm.

The corrosion of prestressing steel strands/tendons has been a major concern in the construction of concrete buildings, bridges, and other structures—especially in cold climates where there is a significant amount of snowfall and use of deicing salts, leading to serious deterioration of concrete structures over time.

The innovative development and use of fibrous composite materials, such as carbon fiber reinforced polymers (CFRP), aramid fiber reinforced polymers (AFRP), and glass fiber reinforced polymers (GFRP), have alleviated the problem of corrosion in many applications.[1] Moreover, these fiber reinforced polymer (FRP) materials, especially CFRP, have other important characteristics, such as high strength- and stiffness-to-weight ratios, a light weight, insensitivity to magnetic effects, ease of handling, and the ability to fabricate laminates or lamina of desired strength and stiffness, or both. Thus, FRP materials have emerged as potential future construction materials, especially for concrete bridge structures and pavement components exposed to deicing salts and aggressive environments.

The technological development and use of post-tensioned concrete box-girder bridges in the United States have progressed at a remarkable rate.[2] In addition, precast, prestressed concrete members are being widely used in the construction of modern bridges due to their construction, structural, and field-application advantages.[3]

Some of the typical advantages of box-beam bridges include the following:

- Small depth compared with other shapes;
- Structural stability and better aesthetic appearance due to monolithic construction;
- Hollow portions inside the box beams, providing an ideal and safe space for gas lines, water pipes, telephone ducts, storm drains, sewers, and other utilities;
- High torsional stiffness, ideal for curved bridges and segmental bridge construction; and
- Low depth-to-span ratios of box beam sections, providing a slender and aesthetically pleasing appearance.[3]

Some of the available literature related to the flexural response of concrete beams prestressed using both bonded and unbonded FRP tendons is described in the following section.

T. Kato and N. Hayashida studied the flexural characteristics of concrete beams prestressed using bonded and unbonded CFRP tendons.[4] They concluded that the failure of concrete beams prestressed with bonded CFRP tendons was due to the brittleness of the beams, whereas the beams prestressed with unbonded CFRP tendons had roughly the same ductility as beams prestressed with steel reinforcing bars.

H. Mutsuyoshi and A. Machida explored the behavior of prestressed

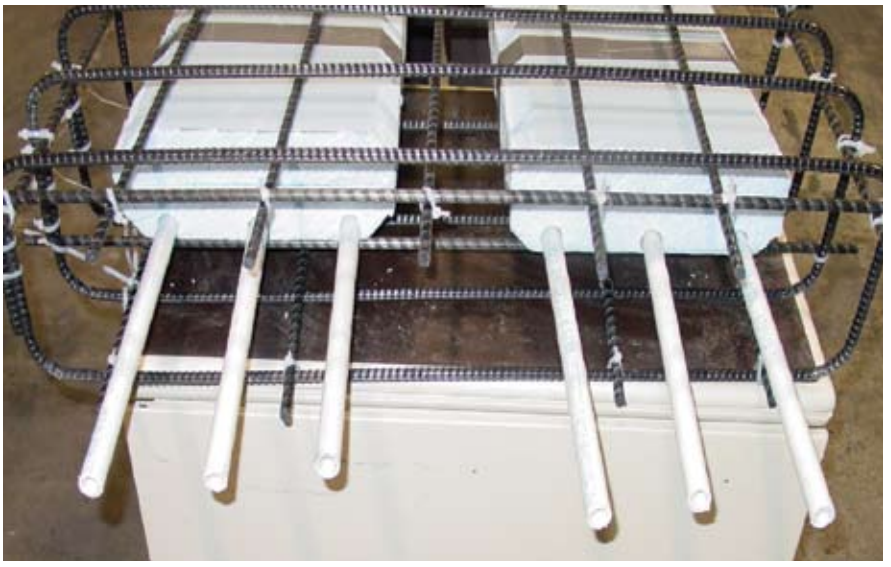

Fig. 2a. Close-up view of carbon fiber reinforced polymer reinforcement cage of box beam BBD-1.

Fig. 2b. Carbon fiber reinforced polymer reinforcement cage for BBD-I placed in the formwork.

concrete beams using FRP as external cable.[5] Based on their experimental investigation, they concluded that the load-deflection responses of beams prestressed with FRP are similar to those prestressed with steel. It was noted that the ductility of FRP-prestressed beams could be improved with the provision of external prestressing.

The flexural behavior of bridges comprising double tees prestressed using bonded and external unbonded, CFRP post-tensioning tendons was studied by Nabil F. Grace and G. A. Sayed under repeated load effects. It was observed that the repeated load has no significant effect on the bridge system.[6] Grace et al. recently evaluated a full-scale double tee bridge beam reinforced and prestressed using bonded and unbonded CFRP/CFCC tendons/strands.[7]

A. Maissen and C. A. M. De Semet compared the behaviors of concrete beams prestressed using CFRP bonded and unbonded tendons with those of beams prestressed with bonded steel strands.[8] They concluded that the flexural capacities of beams prestressed with bonded and unbonded tendons were greater than those of beams prestressed with bonded tendons only.

A. E. Naaman and S. M. Jeong studied the structural ductility of concrete beams prestressed with AFRP, CFRP, and steel strands.[9] They concluded that the beams prestressed with FRP tendons had considerably lower ductility than the beams prestressed with steel strands. A new construction approach for multispan, continuous, CFRP-prestressed concrete bridges demonstrated that external post-tensioning using continuous draped tendons, continuity design of deck slab, and transverse post-tensioning increased the ductility of the bridge system.[10,11]

H. Taniguchi et al. examined the flexural response of concrete beams prestressed using CFRP and AFRP tendons under static and dynamic loadings.[12] They observed that the CFRP and AFRP ropes used as external prestressing strands broke at stress levels equal to 70% and 90% of their ultimate strength, respectively. They also observed that the use of CFRP as transverse reinforcement increased the ductility of the beams. Furthermore, the prestressing cables did not fail, even after two million cycles of repeated loads and experiencing a tension below 50% of their ultimate strength.

Recently, Chee-Khoon Ng has experimentally and theoretically examined the tendon stress and flexural strength of externally prestressed beams and has shown that the beam span has no significant effect on the stress increase in external tendons.[13] From a parametric study using a nonlinear computer program based on a strain-controlled approach, Grace and Shamsher Singh concluded that the double tee beam prestressed using multilayered pretensioning and external post-tensioning CFRP tendons experienced a 26% higher load capacity and 36% lower energy ratio than the beam with non-prestressed, unbonded post-tensioning tendons.[14] Moreover, levels of initial pretensioning and post-tensioning forces significantly affect the flexural response and failure mode of the beam.[14,15]

The objective of the present investigation is to develop and construct precast, prestressed concrete box beams using bonded Diversified Composites Inc. (DCI) tendons and subsequently use them to construct three bridge models whose box beams are additionally prestressed using longitudinal and transverse, unbonded post-tensioning tendons. In addition, the study also measures transfer lengths of DCI ten-

Table 1. Properties of DCI Tendons, MIC C-Bars, and Leadline™ Tendons.

Material Characteristics	Diversified Composites Inc. (DCI) Tendons	Marshall Industries Composites Inc. (MIC) C-Bars Stirrups	Mitsubishi Functional Products Inc. Leadline Tendons
Nominal diameter, d_b in. (mm)	0.374 (9.5)	0.374 (9.5)	0.315 (8)
Cross-sectional area in.^{2} (mm^2)	0.11 (70.9)	0.11 (70.9)	0.071 (46.1)
Specified tensile strength ksi (MPa)	280 (1930)	275 (1896)	330 (2272)
Elastic modulus ksi (GPa)	19,000 (131)	16,000 (110)	21,320 (147)
Maximum elongation %	1.47	1.7	1.5

dons, deflections, strains, and ultimate loads of box-beam bridges. Finally, the analytically predicted flexural response is compared with that of the measured response.

CONSTRUCTION DETAILS

Three bridge models, each consisting of two precast, prestressed concrete box beams, were constructed. The models were designated BBD-I, BBD-II, and BBD-III, depending on the arrangement and forces in the unbonded post-tensioning tendons for prestressing applications. Each of the rectangular concrete box beams used in the construction of the bridge models were 20 ft (6.1 m) long, 38 in. (970 mm) wide, and 9 in. (230 mm) deep.

Figure 1 shows both the cross-sectional details of BBD-I, with a 3-in.-thick (75 mm) concrete deck slab cast over the adjacent prestressed concrete box beams, and the longitudinal section details of BBD-I. The cross and longitudinal sections of the other two bridge models, BBD-II and BBD-III, are the same as those of BBD-I, except that BBD-II was not provided with unbonded post-tensioning tendons and BBD-III was provided with non-prestressed unbonded tendons with their prestressing heads anchored at both ends of the bridge model.

As shown in Fig. 1, each box beam of the bridge model comprised two hollow rectangular portions formed by commercially available Styrofoam™. Each hollow section was 12 in. (300 mm) wide and 4 in. (100 mm) deep. In addition, each box beam was provided with four rectangular transverse diaphragms, one at each end of the beam and two at intermediate sections symmetrically located about beam midspan, to facilitate transverse post-tensioning of the bridge model.

The construction of each box beam required preparation of a CFRP reinforcement cage (**Fig. 2a**). The reinforcement cage consisted of Marshal Industries Composites (MIC) shear stirrups at a spacing of 4 in. (100 mm) to avoid premature shear failure; and six polyvinyl composite (PVC) conduits in the longitudinal direction and four PVC tubes in the transverse directions to pass the longitudinal and transverse post-tensioning tendons, respectively.

Table 1 shows the material properties of the DCI tendons, MIC shear stirrups, and Leadline™ tendons. The prepared reinforcement cage was placed in the formwork for each box beam. It should be noted that an arrangement was made to construct the two box beams for each bridge model simultaneously by constructing their formwork side by side, along with prestressing arrangements (**Fig. 2b**).

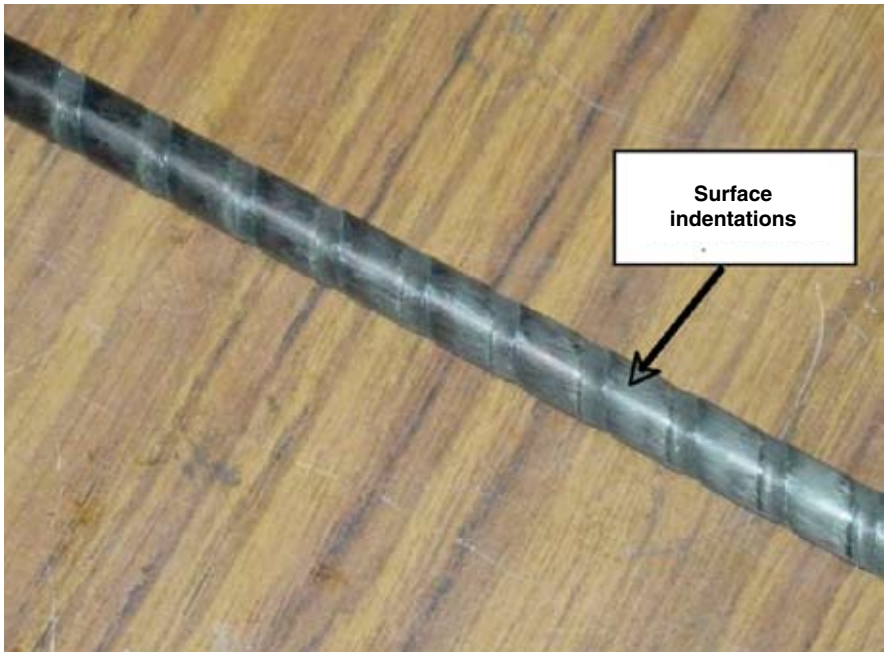

Fig. 3. Closer view of Diversified Composites Inc. reinforcing/prestressing tendon.

Table 2. Prestressing Tendons and Reinforcement Details of the Three Adjacent Box-Beam Bridge Models.

Designated Bridge Model	Number of Box Beams	Designated Box Beam	Type of CFRP Reinforcement		Number of Prestressing Tendons		Number of Flexural Non-Prestressing Rods		Number of Deck Slab Reinforcing Bars	
			Box Beam	Deck Slab	Pretensioned	Unbonded Post-Tensioned	Top	Bottom	Longitudinal	Transverse
BBD-I	2	BP-1	DCI	Leadline	7	6 (4)*	7	4	10	31
		BP-2			7	6 (4)*	7	4		
BBD-II	2	B0-1	DCI	Leadline	7	0 (4)*	7	4	10	31
		B0-2			7	0 (4)*	7	4		
BBD-III†	2	BN-1	DCI	Leadline	7	6 (4)*	7	4	10	31
		BN-2			7	6 (4)*	7	4		

* Values in parentheses represent the number of transverse unbonded tendons, while those outside the parentheses represent the number of longitudinal unbonded tendons.
†Unbonded post-tensioning tendons with prestressing heads were anchored at both ends of the bridge model without any force.

After the placement of the reinforcement cage in the formwork, seven DCI pretensioning tendons were passed through the cage and abutment for subsequent prestressing. **Figure 3** shows a closer view of a CFRP DCI tendon. In addition, seven non-prestressing DCI tendons at the top and four non-prestressing tendons at the level of pretensioning tendons were also tied to the reinforcement cage. The top non-prestressing tendons were provided to prevent cracking due to shrinkage stresses and handling operations. Commercially available zip ties were used to tie the reinforcement cage together.

To provide the required 2 in. (50 mm) concrete cover at the bottom of the beam, 4-in.-diameter (100 mm) plastic circular chairs were provided in the formwork. Before placing concrete in the formwork, the pretensioning tendons were first instrumented with strain gauges as described in the section "Instrumentation and Test Setup."

Prestressing

All six box beams were prestressed using seven pretensioning DCI tendons (**Table 2**). A wedge-based anchorage system was used for prestressing application. Each tendon was stressed to an average of 10 kip (45 kN) force, thereby applying 70 kip (310 kN) of prestressing force to each box beam. The prestressing system (**Fig. 4**) consisted of a long stroke center-hole jack, a hydraulic pump with pressure gauge, prestressing chair, a threaded steel rod, and a coupler. The jacking force was monitored using the pressure of the hydraulic pump and the load cells located at the tendon's dead end.

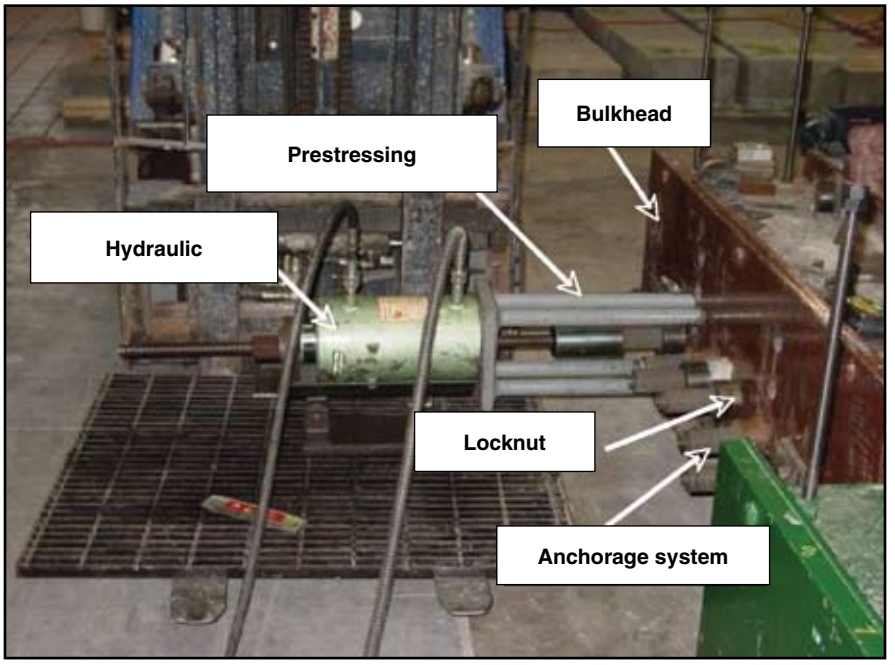

Fig. 4. Pretensioning system consisting of center-hole hydraulic jack.

After pretensioning, concrete was placed in the formwork (**Fig. 5**) to fabricate two box beams at a time with four bulkheads fixed to the floor (Fig. 2a, 2b). The box beams were wet cured using soaked burlap for seven days. The shear stirrups protruded from the top concrete surface of the box beams to provide shear connection with the deck slab in the integrated adjacent box-beam bridge construction (**Fig. 6, 7**).

When the concrete achieved the desired compressive strength, a hand-held saw was used to cut the tendons and transfer the prestress force to the concrete section. The 28-day compressive strengths of concrete for the box beams of bridge models BBD-I, BBD-II, and BBD-III were 7.3 ksi, 7.9 ksi, and 7.8 ksi (50.3 kN, 54.5 kN, and 53.8 kN), respectively.

Construction of Adjacent Box-Beam Bridge Models

Individual precast, prestressed concrete box beams were moved to the testing area within the loading frame and were placed side by side with simple supports at their ends. The adjacent arrangement of box beams provided a solid platform for the initial post-tensioning application. The gap between the two adjacent box beams in each bridge model was filled with a grout (Five Star Structural Concrete) (Fig. 6). The 7-day and 28-day compressive strengths of grout were 9000 psi (62 MPa) and 10,000 psi (69 MPa), respectively.

After curing of the grout, an initial transverse post-tensioning force was applied in each of the four transverse post-tensioning tendons passing through the corresponding transverse diaphragms in the adjacent box beams (Fig. 7). Initial transverse post-tensioning consisted of applying 50% of the design transverse post-tensioning force (10 kip [45 kN]).

After initial transverse post-tensioning, an initial longitudinal post-tensioning force was also applied to the unbonded longitudinal tendons. The initial longitudinal post-tensioning force was about 10% of the total design post-tensioning force (20 kip [90 kN]) in these tendons.

These initial post-tensioning forces were necessary to maintain the structural integrity of the two adjacent box beams and to prevent differential movement during casting of the deck slab and application of external loads. Final transverse and longitudinal post-tensioning forces were applied after construction of the deck slab.

Construction of Deck Slab

Before the construction of the deck slab, a reinforcement cage fabricated with 0.3-in.-diameter (8 mm) Leadline tendons in the form of a rectangular grid were placed over the protruded stirrups in the formwork (**Fig. 8**). A 3-in.-thick (76 mm) concrete deck slab was cast in the prepared formwork. The 28-day compressive strengths of deck slab concrete for BBD-I, BBD-II, and BBD-III were 7.8 ksi, 7.9 ksi, and 7.9 ksi (53.8 MPa, 54.5 MPa, and 54.5 MPa), respectively.

Fig. 5. Placement of concrete in the formwork after pretensioning of tendons.

The final transverse and longitudinal post-tensioning forces, constituting about 50% and 90% of their corresponding design values, were applied after the deck slab achieved the desired compressive strength. **Figure 9** shows the final transverse post-tensioning of BBD-I after casting of the concrete deck slab. Table 2 presents details of the prestressing tendons and reinforcement provided in the box beams and deck slab of each bridge model.

INSTRUMENTATION AND TEST SETUP

Demec points were used to measure concrete strain at the two ends of the box beams to determine the transfer length at the time the prestress force was transferred to the concrete. Mea-

Fig. 6. Grouting of longitudinal joint between two box beams.

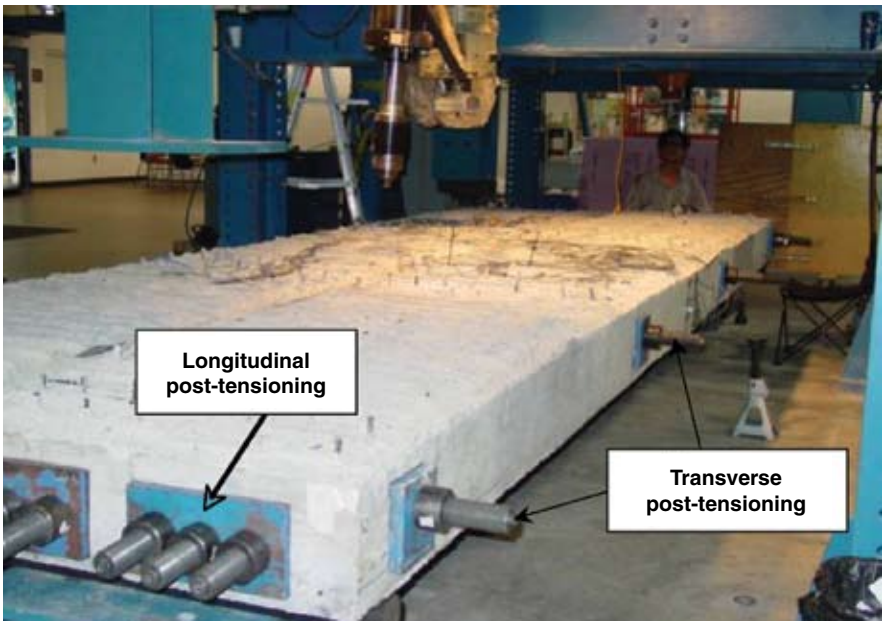

Fig. 7. Model BBD-I partially prestressed with transverse and longitudinal post-tensioning tendons before placing the concrete deck slab.

Fig. 8. Bridge model BBD-I before the concrete deck slab casting.

surements were taken manually before and after the release of pretensioning forces to measure the strain using Demec gage ID-C112M, with an accuracy of 5×10^{-5} in. (127×10^{-5} mm).

To measure strain during external loading, six strain gauges were installed on either side of the bridge system at midspan (**Fig. 10**). The bottom and top strain gauges were installed approximately 1 in. (25 mm) from the corresponding nearest edge, while the remaining four strain gauges were equally spaced over the 10 in. (250 mm) depth of the bridge model. In addition, five strain gauges were installed at the top surface of the deck slab.

The top surface strain gauges were symmetrically placed about the longitudinal mid-axis of the bridge model. To measure the deflection of the bridge model, two linear motion transducers were installed at midspan, while one linear motion transducer was installed at each quarter-span section. Load cells installed at the dead end of the longitudinal and transverse post-tensioning tendons measured the post-tensioning forces in these tendons.

All the sensors installed in the box beams, which measured strains and forces in the pretensioning tendons, and strain gauges installed on non-prestressing tendons were operational for acquisition of data during the ultimate load test. To collect and store data, all strain gauges, load cells, and linear motion transducers were connected to the data acquisition system. To experimentally record the load capacity, deflection, strain, and post-tensioning forces in the unbonded tendons, the three bridge models were loaded to failure at a rate of approximately 6 kip/min (26.7 kN/min).

ANALYTICAL APPROACH

To analytically predict the deflection, strain, and forces in unbonded post-tensioned tendons, a nonlinear analysis of the bridge models was performed using a computer program based on a unified design approach.[14,15] The analysis was performed only for a single box-beam because of the symmetry of bridge systems with respect to the boundary conditions and applied load.

To predict the forces in the unbonded post-tensioning tendons, however, the axial deformation of the entire box beam was considered instead of using the ultimate bond reduction coefficient of Naaman and Alkhairi.[16] The computer program incorporated a parabolic stress-strain relationship for the concrete and a linear stress-strain relationship for the CFRP tendons. The compressive force in the concrete is based on the equivalent rectangular stress block factors.[14]

Equivalent stress block factors depend on the level of extreme compression fiber strain and the parabolic stress-strain relationship of concrete. The resultant compression force comprises forces in the concrete and CFRP non-prestressed tendons within the compression zone. The incremental strain-controlled approach was used to predict the neutral axis depth, strains, and curvatures at preselected sections

along the length of a box beam of a particular bridge model.

Midspan deflections were computed by integrating the curvature of the box beam along its length. The average axial deformation of the bridge system at the level of the post-tensioned tendon was evaluated by integrating the axial strain along the length of the box beam at the unbonded tendons level. The product of the elastic modulus of the unbonded tendon, the average axial strain, and the effective cross-sectional area of the unbonded tendons is reported as forces in the corresponding tendon. Details of design equations for under-reinforced and over-reinforced box beams can be found elsewhere.[14]

TEST RESULTS AND DISCUSSION

In this section, transfer lengths, failure modes of the three bridge models, and experimental verification of analytical results are presented.

Transfer Lengths

The transfer length equations recommended by ACI 318, Grace, and Zou are given as Eq. 1, 2, and 3, respectively.[17–19]

$$L_t = \frac{f_{pi} d_b}{20} \qquad \text{(Eq. 1)}$$

$$L_t = \frac{f_{pi} d_b}{\alpha_t f_{ci}'^{0.67}} \qquad \text{(Eq. 2)}$$

$$L_t = \frac{480 d_b}{\sqrt{f_{ci}'}} \qquad \text{(Eq. 3)}$$

where

d_b = nominal diameter of tendon/strand (mm)
f_{pi} = prestress force at transfer (MPa)
f_{ci}' = the compressive strength of concrete at transfer (MPa)
α_t = transfer length coefficient, where $\alpha_t = 1.95$ for CFRP Leadline tendons

Note: DCI tendons are similar to CFRP Leadline tendons; hence, α_t was taken equal to 1.95 for computation of transfer length.

Table 3 presents the transfer lengths for DCI tendons measured from the six box beams used in the construction of three adjacent box-beam bridge models. The transfer lengths are based on the saw-cut release of prestressing forces seven days after the concrete was cast. The transfer lengths were determined from the strain distribution along the length of the box beam near the ends using 95% average maximum strain method for 100% release of prestressing forces.[18]

Fig. 9. Transverse post-tensioning of bridge model BBD-I after casting of the concrete deck slab.

In Table 3, BP-1 and BP-2 refer to box beams 1 and 2 of the bridge model prestressed using both the pretensioning and unbonded post-tensioning tendons; B0-1 and B0-2 are box beams of the bridge model without longitudinal, unbonded post-tensioning tendons; and BN-1 and BN-2 are box beams of the bridge model provided with non-prestressed, unbonded post-tensioning tendons.

Fig. 10. Test setup of box-beam bridge models.

Table 3. Transfer Lengths of DCI Pretensioning Tendons of Box-Beam Bridge Model.

Designated Bridge Model	Designated Beams	Average Prestress at Transfer, f_{pi}, ksi (MPa)	Concrete Strength at Transfer, f'_{ci}, ksi (MPa)	Measured Transfer Lengths, L_t, in. (mm)			Calculated Transfer Lengths, L_t, in. (mm)		
				Live End	Dead End	Average	Eq. 1 (ACI 318)	Eq. 2 (Grace)	Eq. 3 (Zou)
BBD-I	BP-1	91.18 (628.55)	4.9 (33.79)	9 (229)	10 (254)	9.5 (241)	11.8 (299)	11.4 (290)	30.9 (785)
	BP-2	92.33 (636.59)		12 (305)	10 (254)	11 (279)	11.9 (302)	12.1 (306)	30.9 (785)
BBD-II	B0-1	96.43 (664.87)	5.05 (34.82)	10 (254)	11 (279)	10.5 (267)	12.4 (316)	11.8 (300)	30.4 (773)
	B0-2	93.03 (641.41)		10 (254)	12 (305)	11 (279)	12 (305)	11.4 (290)	30.4 (773)
BBD-III	BN-1	91.76 (632.66)	5.1 (35.16)	13 (330)	11 (279)	12 (305)	11.8 (301)	11.2 (284)	30.3 (769)
	BN-2	90.36 (623.00)		11 (279)	11 (279)	11 (279)	11.7 (296)	11 (280)	30.3 (769)

It is observed that the average values of the measured transfer lengths of 0.374-in.-diameter (9.5 mm) DCI tendons are from 25 to 32 times the nominal diameter of tendons. In Table 3, the calculated transfer lengths obtained using the ACI 318, Grace, and Zou equations are presented.[17–19]

The measured transfer lengths shown in Table 3 are close to those predicted by the ACI and Grace equations; however, these are significantly lower than those predicted by Zou.[17–19] These results suggest that the effect of prestress force at transfer should be taken into consideration along with concrete strength for predicting the transfer length of pretensioning tendons, contradicting the concluding remarks of Zou.[19]

Zou reported that for all practical purposes, the effect of prestress force on transfer length of tendons can be neglected and the transfer length should solely be based on Eq. 3 (modified version of BS 8110, BSI).[19,20] From Table 3, it can be predicted that the average values of transfer lengths calculated by the ACI, Grace, and Zou equations are in the range of 31.1 to $33d_b$, 30 to $32.4d_b$, and 80.9 to $82.5d_b$, respectively. Here, d_b refers to nominal diameter of DCI tendons.[17–19]

Failure Mode of Bridge Model

To predict the ultimate load response and failure modes of the bridge models, all three bridge models were subjected to ultimate load response after subjecting each bridge model to a number of loading and unloading cycles. The experimental and analytical deflections, strains, and forces in unbonded tendons are presented and discussed in the next section.

As shown in **Fig. 11**, **12**, and **13**, all three bridge models experienced flexural failure. **Table 4** shows the load corresponding to the first crack and ultimate loads of the three bridge models. The BBD-I with box beams prestressed using both pretensioned and unbonded post-tensioning tendons had the highest ultimate load, while the model without longitudinal post-tensioned tendons (BBD-II) had the lowest ultimate load.

The failure of BBD-I containing box beams prestressed using pretensioned and unbonded post-tensioning tendons was initiated due to the crushing of concrete before rupture of pretensioning tendons. The failures of BBD-II and BBD-III were initiated by rupture of pretensioning tendons before crushing of concrete. The delayed crushing of concrete in BBD-III, however, resulted in higher absorption of inelastic

Table 4. Details of Cracking, Failure Loads, and Energy Ratios.

Designated Bridge Models	Cracking Load kip (kN)	Ultimate Load kip (kN)	Energy Ratio (%)	Primary Mode of Failure
BBD-I	24 (106.8)*	146 (649.7)	25.0	Crushing of concrete
BBD-II	17 (75.7)*	127 (565.15)	46.9	Rupture of bonded pretensioning tendons
BBD-III	18 (80.1)*	128 (569.6)	48.5	Rupture of bonded pretensioning tendons

*Results are based on first cracking in one of the box beams of the box-beam bridge model.

energy and, hence, an enhanced energy ratio (Table 4).

These failure modes were expected because BBD-I was over-reinforced, while BBD-II and BBD-III were under-reinforced.[14] It should be noted that the definitions of over- or under-reinforced sections depend on the total level of prestressing forces in a member.

Experimental Verification

In this section, deflections, strains, and forces in unbonded post-tensioning tendons obtained from experimental testing and analytical study are presented and discussed for the three bridge models. **Figure 14** shows the load-deflection response of BBD-I up to the ultimate failure load. It is observed that the analytical and experimental load deflection responses are in fair agreement, except that the analytical strength of BBD-I is about 4% lower than the experimental strength.

For a particular load, the experimental deflection is slightly larger than the analytical deflection due to the bridge models' being subjected to loading-unloading cycles before the ultimate load test. The loading-unloading cycles were necessary to compute the energy ratio associated with the bridge model. The ductility of each bridge model was evaluated by calculating the released elastic energy and absorbed inelastic energy at the time of failure. The energy ratio is a measure of ductility and is determined by computing the ratio of inelastic energy absorbed to the total energy of the bridge model. The experimental ultimate load and energy ratio (Table 4) of BBD-I are 146 kip (650 kN) and 25%, respectively.

Figure 15 shows the load versus extreme compression fiber strain response observed from experimental and analytical study of BBD-I. It is shown that the analytical compressive strains and corresponding experimental strains are very close throughout the loading up to ultimate failure.

Similarly, **Fig. 16** shows the forces in the longitudinal, unbonded post-tensioning tendons of BBD-I. As in the case of deflection and compressive strain, analytical values of forces in these tendons are very close to the experimentally observed maximum forces in the post-tensioned tendons.

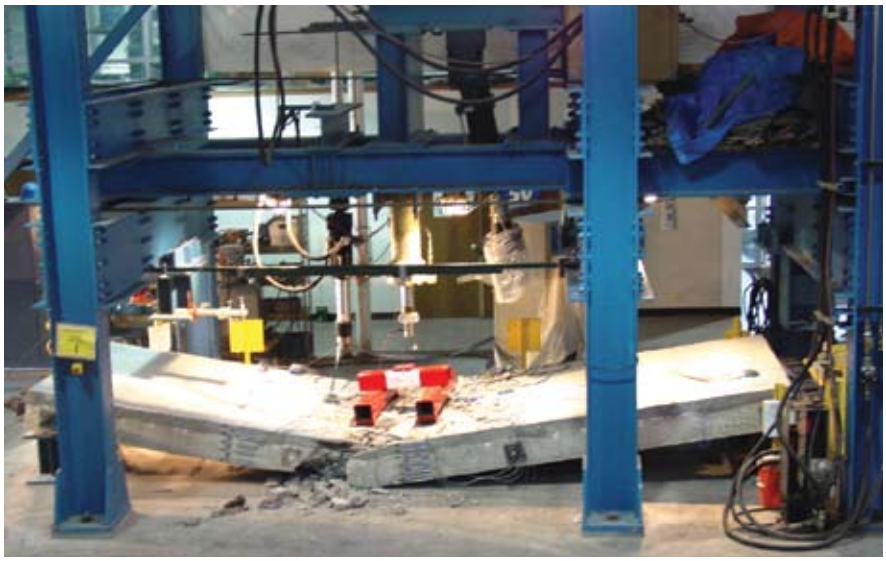

Fig. 11. Failure of bridge model BBD-I.

Fig. 12. Failure of bridge model BBD-II.

Fig. 13. Failure of bridge model BBD-III.

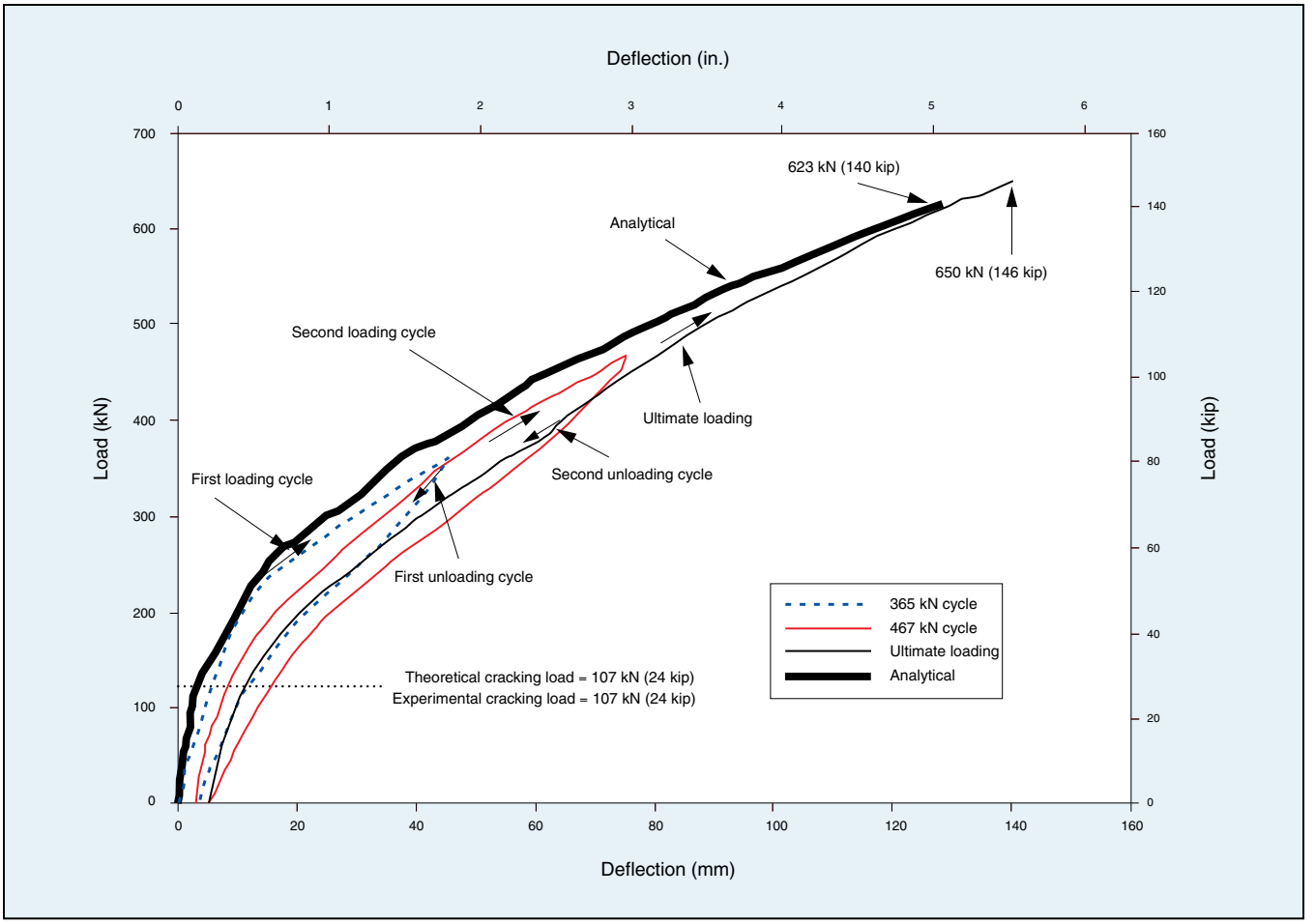

Fig. 14. Load-deflection at midspan of bridge model BBD-I. Note: 4.45 kN = 1 kip; 25.4 mm = 1 in.

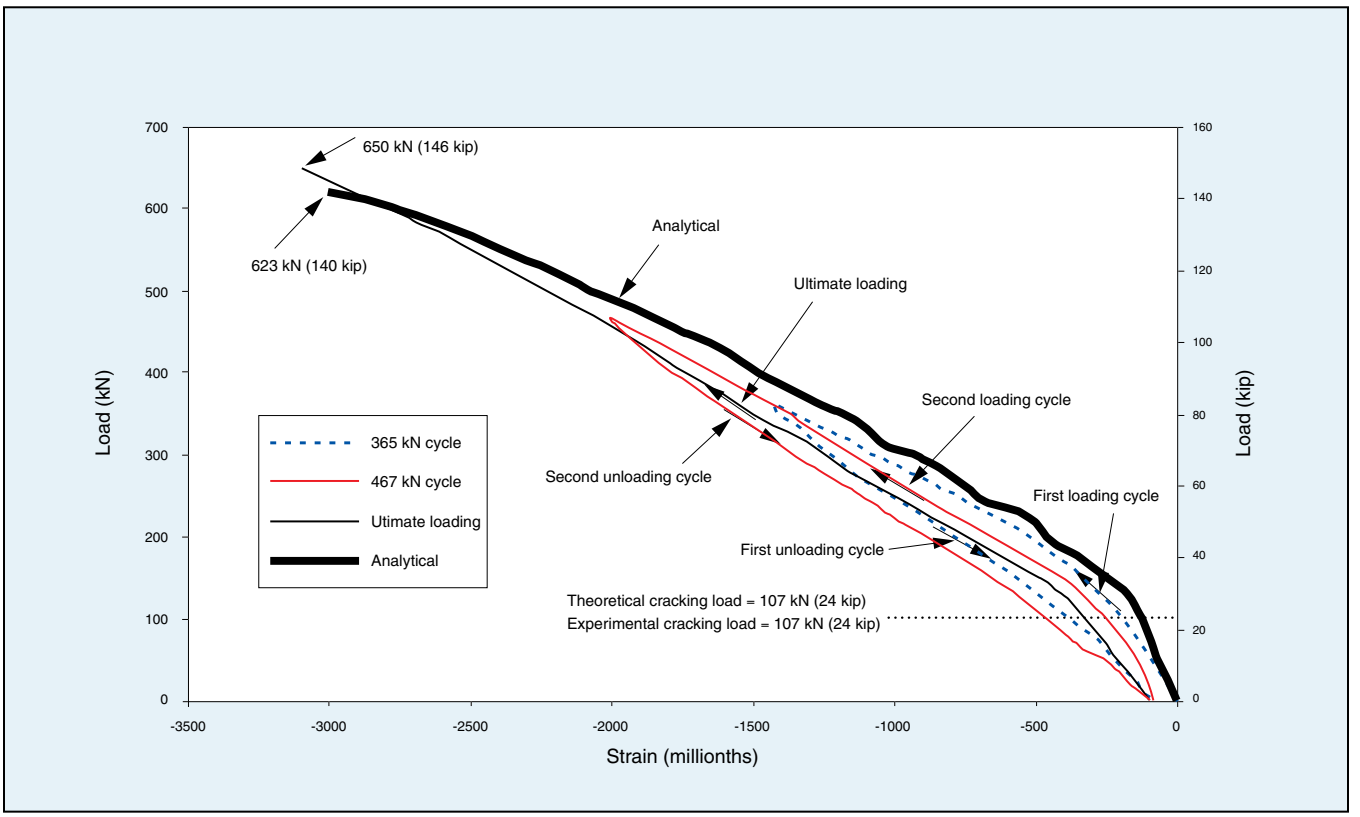

Fig. 15. Load versus longitudinal strain measured at top of deck slab of bridge model BBD-I. Note: 4.45 kN = 1 kip.

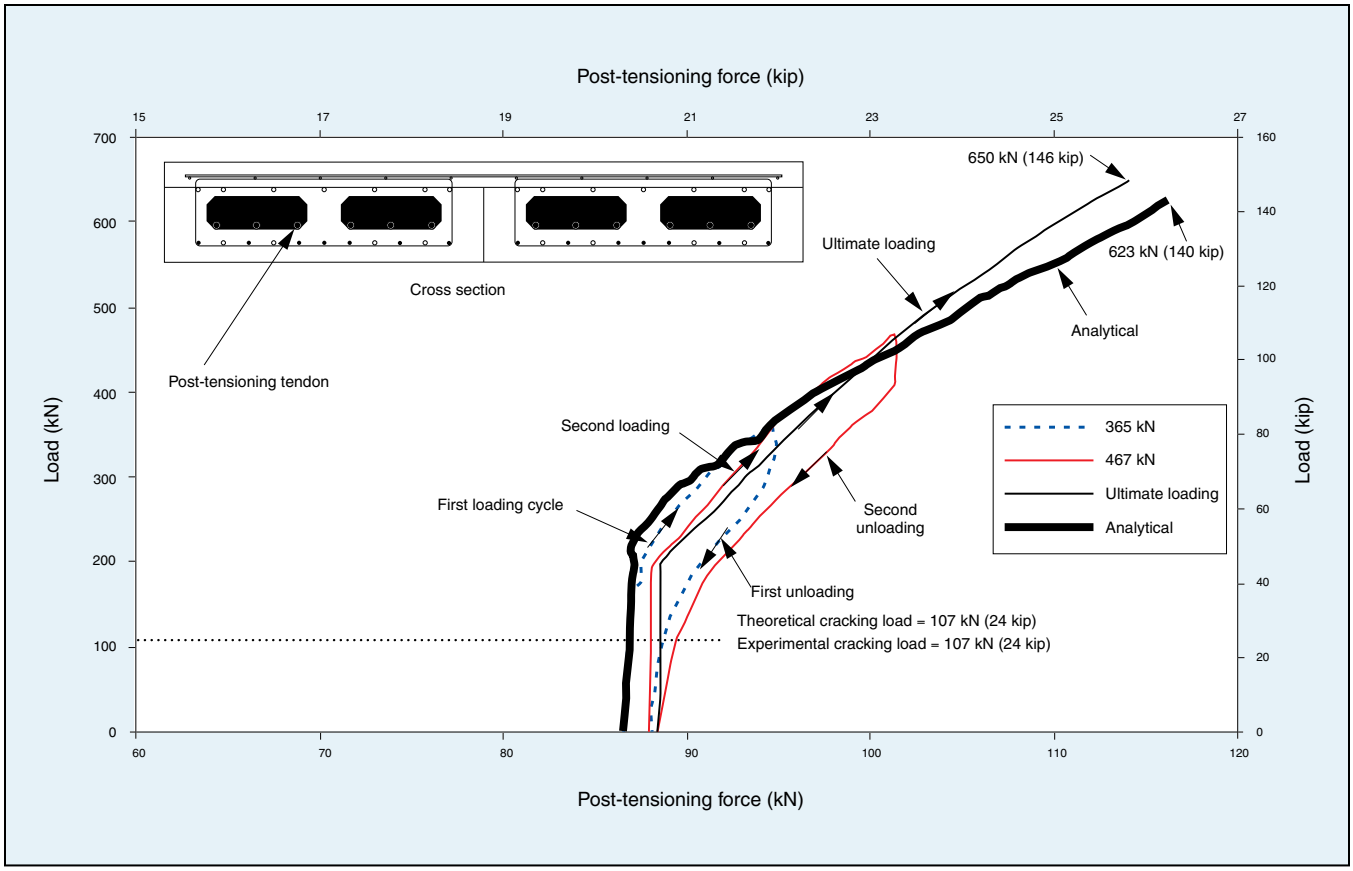

Fig. 16. Load versus force in a typical longitudinal, unbonded tendon carrying maximum post-tensioning force in bridge model BBD-I. Note: 4.45 kN = 1 kip.

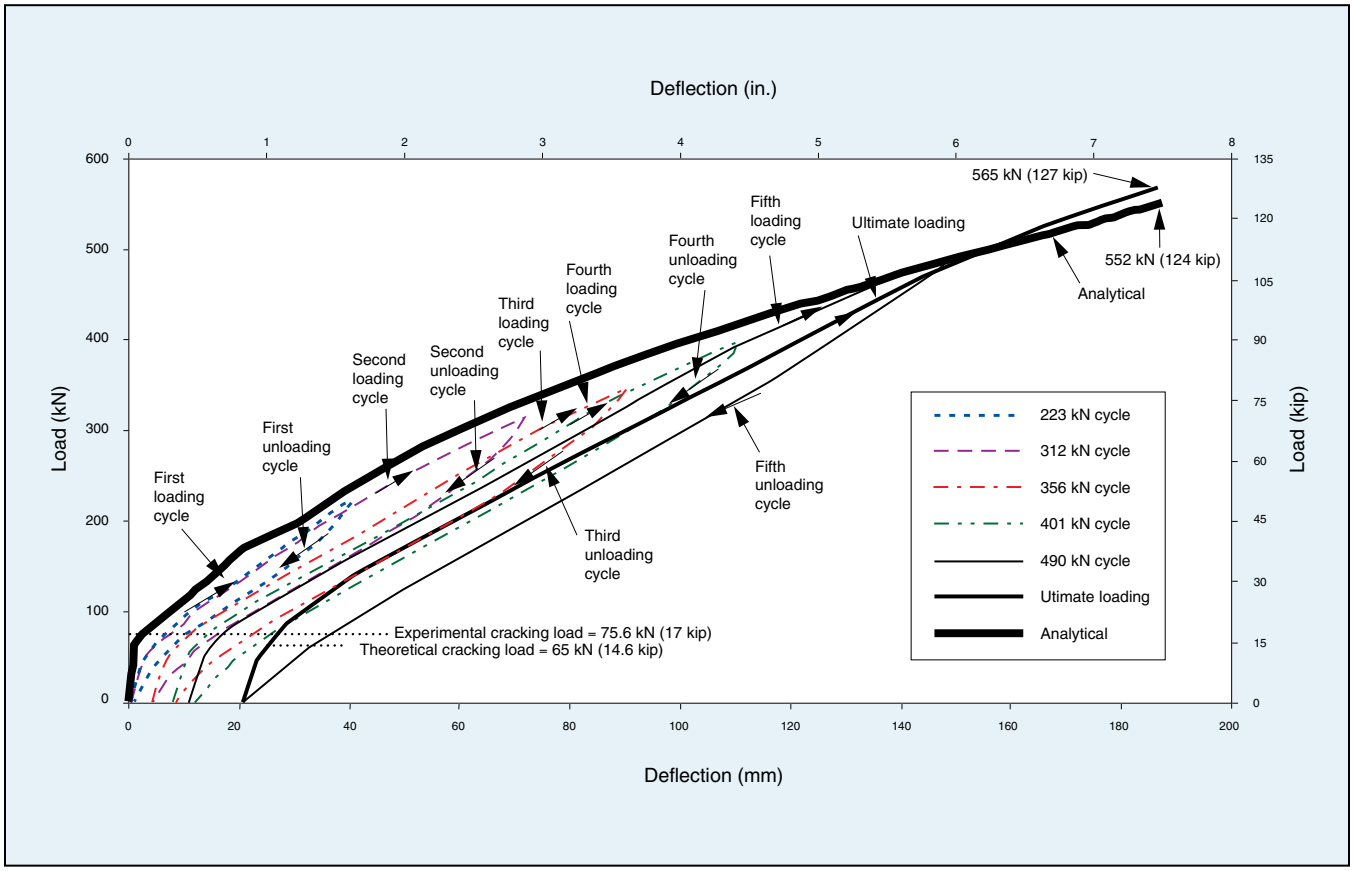

Fig. 17. Load-deflection at midspan of bridge model BBD-II. Note: 4.45 kN = 1 kip; 25.4 mm = 1 in.

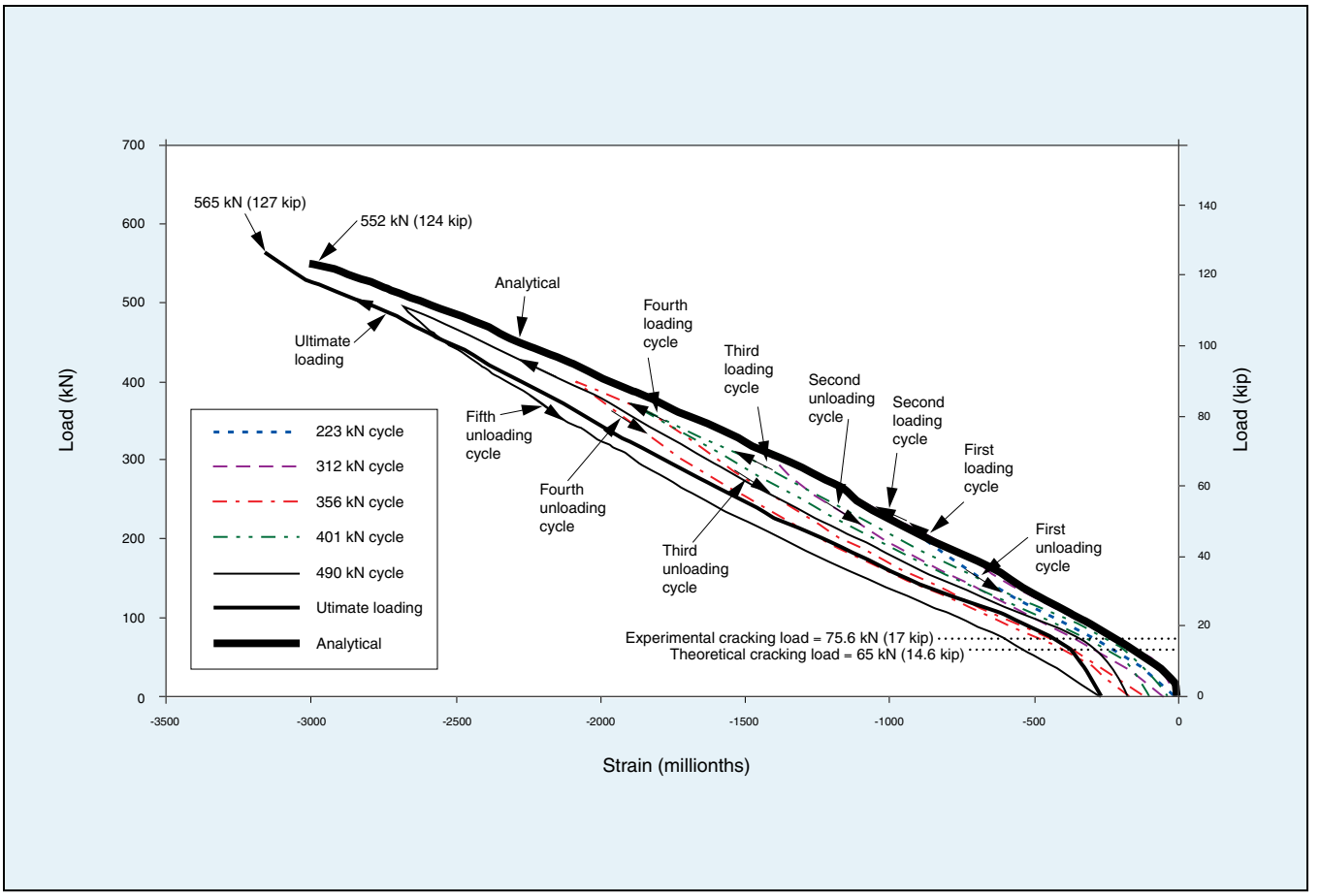

Fig. 18. Load versus longitudinal strain measured at the top of deck slab of bridge model BBD-II. Note: 4.45 kN = 1 kip.

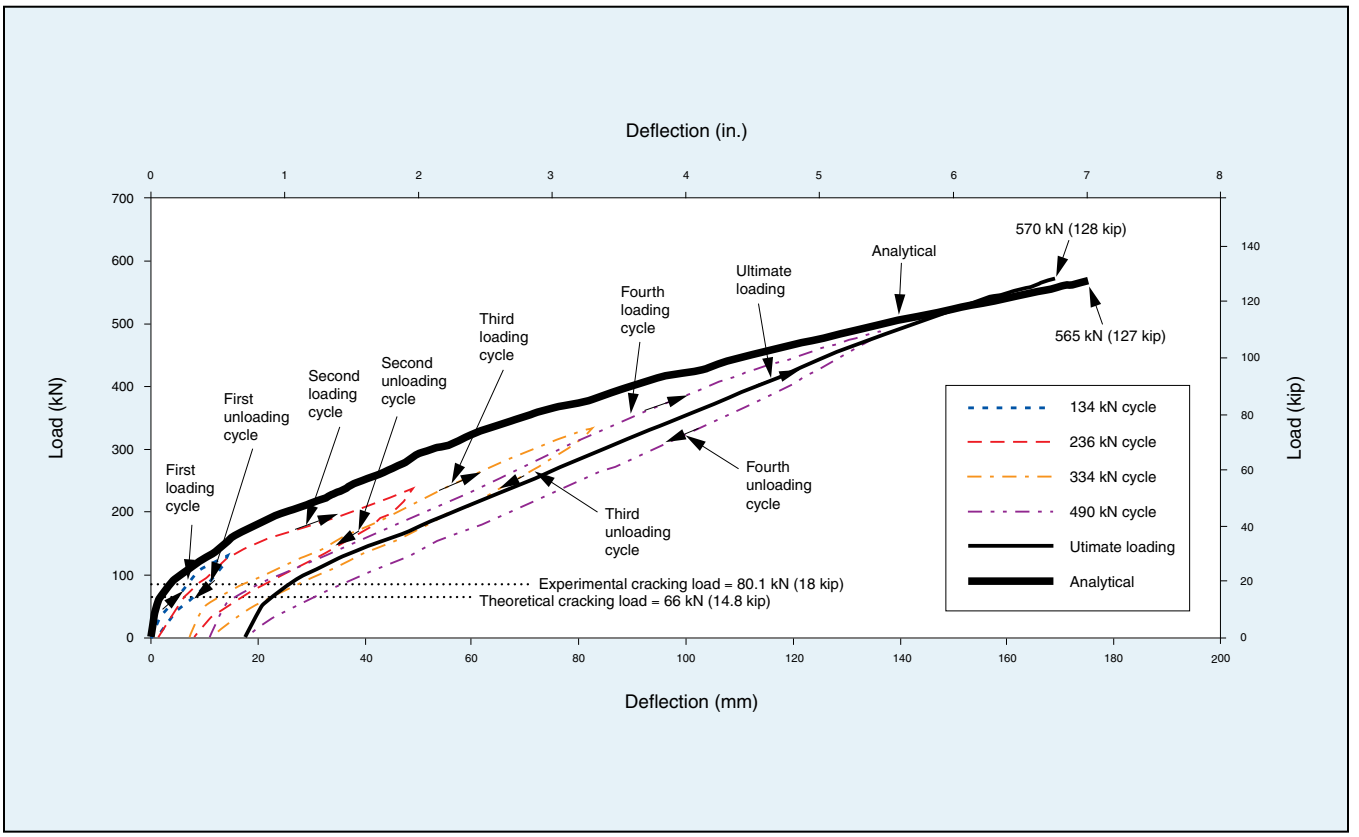

Fig. 19. Load-deflection at midspan of bridge model BBD-III. Note: 4.45 kN = 1 kip; 25.4 mm = 1 in.

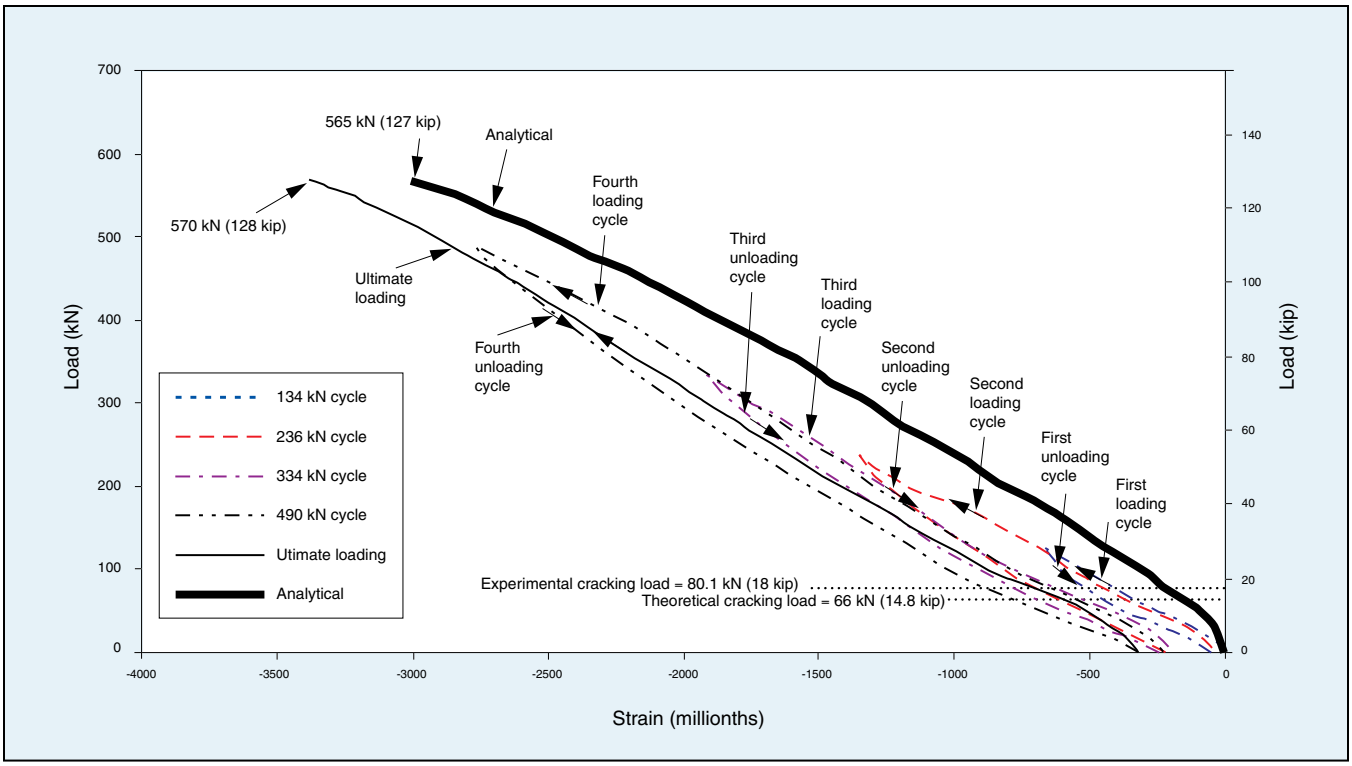

Fig. 20. Load versus longitudinal strain measured at top of deck slab of bridge model BBD-III. Note: 4.45 kN = 1 kip.

It should be noted that the variation in the forces of transverse unbonded post-tensioned tendons was negligible and, hence, is not presented here.

The load versus deflection and compressive strain responses for BBD-II are shown in **Fig. 17** and **18**, respectively. As mentioned previously, BBD-II was not provided with longitudinal, unbonded post-tensioning tendons. Similar to the case of BBD-I, analytical and experimental deflections and compressive strains of BBD-II are close in agreement.

Successive loading-unloading cycles applied to BBD-II, however, led to higher residual deformation compared with that observed for BBD-I. As expected, the strength of BBD-II was about 13% lower than that of BBD-I. The lower strength of BBD-II is attributed to the absence of longitudinal, unbonded post-tensioning tendons and prestressing tendons.

The combined prestressing using pretensioning and unbonded post-tensioning tendons resulted in the higher strength of BBD-I, with about 22% lower deflection than BBD-II at the ultimate load. The energy ratio of BBD-I, however, was about 22% lower than that of BBD-II (Table 4). These results confirm the experimental and analytical findings and concluding remarks of Grace and Singh.[14]

Similar to the case of BBD-I, the analytical and experimental deflections **(Fig. 19)**, strains **(Fig. 20)**, and forces in unbonded post-tensioning tendons **(Fig. 21)** of BBD-II are close in agreement. The difference, however, in analytical and experimental deflections and strains is slightly large for BBD-III (provided with non-prestressed, longitudinal, unbonded post-tensioning tendons), but the analytical and experimental values of post-tensioning forces are very close. Note that there is no significant difference in the load-deflection response of BBD-II and BBD-III. This is attributed to the proximate location of non-prestressed, unbonded tendons of BBD-III to the box beam's neutral axis.

CONCLUSIONS

In general, CFRP tendons provide a very satisfactory means for prestressing box beams, both for structural strength and corrosion prevention purposes. Furthermore, based on the results of this investigation, several conclusions can be drawn.

The average value of the measured transfer lengths of the 0.374-in.-diameter (9.5 mm) DCI tendons varied from 25 to 32 times the nominal diameter of tendons. The average values of transfer lengths calculated by Grace, ACI, and Zou, however, are in the range of 31 to 33, 30 to 32, and 81 to 83 times the nominal tendon diameter (d_b), respectively.

In general, the analytical and experimental values of deflections, strains, and forces in the unbonded tendons of BBD-I, BBD-II, and BBD-III are in close agreement. This result signifies the accuracy of the strain-controlled approach to analyze CFRP reinforced, adjacent, box-beam bridge models, according to the findings of Grace and Singh.[14]

The cracking and ultimate loads of BBD-I were greater than those of BBD-II and BBD-III. This is attributed to the fact that BBD-I was prestressed using both the pretensioning and unbonded post-tensioning tendons, whereas BBD-II and BBD-III were prestressed with only pretensioning tendons, except that the non-prestressed, unbonded post-tensioning tendons were installed in BBD-III, with their prestressing heads anchored at both

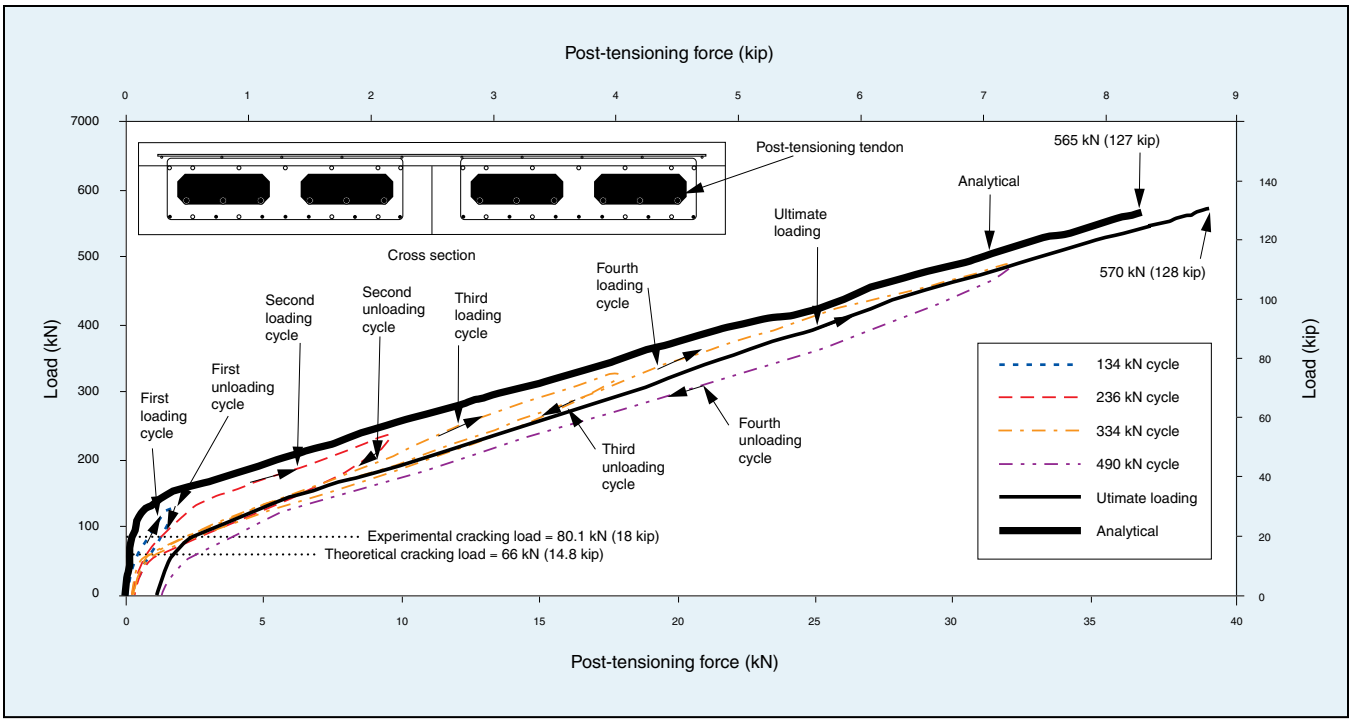

Fig. 21. Load versus force in a typical longitudinal, unbonded tendon carrying maximum post-tensioning force in bridge model BBD-III. Note: 4.45 kN = 1 kip.

ends of the bridge model.

There was no significant difference in load-deflection responses between BBD-II and BBD-III. BBD-II and BBD-III, however, experienced larger deflection compared with BBD-I at ultimate failure, which is attributed to the absence of longitudinal post-tensioning forces. These responses confirm the concluding remarks and recommendations of earlier investigations that the prestressing of the bridge models/girders using both the pretensioning and unbonded post-tensioning tendons could significantly increase their load-carrying capacity, provided that the level of prestressing in pretensioning and unbonded post-tensioning tendons is kept from 0.3 to 0.6 times the specified strength of tendons.

As expected, all three bridge models experienced flexural failure. The failure of BBD-I, prestressed using pretensioning and unbonded post-tensioning tendons, was initiated by the crushing of concrete followed by the rupture of pretensioning tendons. The failure of BBD-II (prestressed using pretensioning tendons and without post-tensioning tendons) and BBD-III (prestressed using pretensioning tendons with non-prestressed, unbonded post-tensioning tendons installed with their heads anchored at both ends of the bridge), however, was initiated by rupture of pretensioning tendons before crushing of concrete.

BBD-I resulted in a lower ductility compared with the ductility of BBD-II and BBD-III. The energy ratio of BBD-III was about 1.94 times that of BBD-I, while it was about 3.4% higher than that of BBD-II.

RECOMMENDATIONS

The proposed design approach can be used for the design of box-beam bridges prestressed using bonded pretensioning and unbonded post-tensioning tendons arranged in vertically distributed layers along with non-prestressed tendons with any combination of material characteristics.

Because both CFRP tendons and concrete materials are brittle in nature, further research is required to study different over-reinforced bridge sections to ensure significant warning before the ultimate collapse of the structure.

From the results of the conducted research, it is clear that an over-reinforced section cannot be considered ductile. Therefore, extensive research is recommended to establish a quantitative relationship between the balanced ratio and the actual reinforcement ratio of box-beam sections that would yield sufficient warning before ultimate collapse.

ACKNOWLEDGMENTS

This investigation was supported by a consortium of the National Science Foundation (Grants No. CMS 0408593 and CMS 0533260), the Concrete Research Council of the American Concrete Institute, and Diversified Composites Inc.

This experimental program was made possible through the efforts of several research associates, and graduate and undergraduate students. The contributions of Y. Tokal, A. Abdel-Mohti, M. Iskander, M. Labib, C. Elder, and A. Weller are highly appreciated.

Last, the authors express their gratitude to the *PCI Journal* reviewers for their constructive comments.

REFERENCES

1. ACI Committee 440, 1996, *State-of-the-Art Report on Fiber Reinforced Plastic (FRP) Reinforcement for Concrete Structures* (ACI 440R-96), American Concrete Institute, Farmington Hills, MI, 65 pp.
2. Hindi, A., MacGregor, R., Kreger, M.

E., and Breen, J. E., 1995, "Enhancing Strength and Ductility of Post-tensioned Segmental Box Girder Bridges," *ACI Structural Journal*, V. 92, No. 1, January–February, pp. 33–44.
3. Taly, N., 1998, *Design of Modern Highway Bridges*, McGraw Hill Companies Inc., New York, NY, pp. 382–487.
4. Kato, T. and Hayashida, N., 1993, *Flexural Characteristics of Prestressed Concrete Beams with CFRP Tendons*, (ACI SP-138), American Concrete Institute, Farmington Hills, MI, pp. 419–440.
5. Mutsuyoshi, H. and Machida, A., 1993, *Behavior of Prestressed Concrete Beams Using FRP as External Cable* (ACI SP-138), American Concrete Institute, Farmington Hills, MI, 1993, pp. 401–418.
6. Grace, N. F. and Sayed, G. A., 1997, "Behavior of Externally/Internally Prestressed Composite Bridge System," Third International Symposium on Non-Metallic (FRP) Reinforcement for Concrete Structures, V. 2, Sapporo, Japan, pp. 671–678.
7. Grace, N. F., Enomoto, T., Abdel-Sayed, G., Yagi, K., and Collavino, L., 2003, "Experimental Study and Analysis of a Full-Scale CFRP/CFCC Double-Tee Bridge Beam," *PCI Journal*, V. 48, No. 4, July–August, pp. 120–139.
8. Maissen, A. and De Semet, C. A. M., August 1995, "Comparison of Concrete Beams Prestressed with Carbon Fiber-Reinforced Plastic and Steel Strands," Non-Metallic (FRP) Reinforcement for Concrete Structures, Second International RILEM Symposium (FRPRCS), Ghent, Belgium, pp. 430–439.
9. Naaman, A. E. and Jeong, S. M., August 1995, "Structural Ductility of Concrete Beams Prestressed with FRP Tendons," Non-Metallic (FRP) Reinforcement for Concrete Structures, Second International RILEM Symposium (FRPRCS), Ghent, Belgium, pp. 379–386.
10. Grace, N. F., 2000, "Response of Continuous CFRP Prestressed Concrete Bridges Under Static and Repeated Loadings," *PCI Journal*, V. 45, No. 6, November–December, pp. 84–102.
11. Grace, N. F., Enomoto, T., and Yagi, K., 2002, "Behavior of CFCC and CFRP Leadline Prestressing Systems in Bridge Construction," *PCI Journal*, V. 47, No. 3, May–June, pp. 90–103.
12. Taniguchi, H., Mutsuyoshi, H., Kita, T., and Machida, A., 1997, "Flexural Behavior of Externally Prestressed Concrete Beams Using CFRP and Aramid Rope Under Static and Dynamic Loading," Third International Symposium on Non-Metallic (FRP) Reinforcement for Concrete Structures proceedings, V. 2, Sapporo, Japan, pp. 783–790.
13. Ng, Chee-Khoon, 2003, "Tendon Stress and Flexural Strength of Externally Prestressed Beams," *ACI Structural Journal,* V. 100, No. 5, September–October, pp. 644–653.
14. Grace, N. F. and Singh, S. B., 2003, "Design Approach for Carbon Fiber-Reinforced Polymer Prestressed Concrete Bridge Beams," *ACI Structural Journal*, V. 100, No. 3, May–June, pp. 365–376.
15. Grace, N. F., Singh, S. B., Shinouda, M. M., and Mathew, S. S., 2004, "Flexural Response of CFRP Prestressed Concrete Box Beams for Highway Bridges," *PCI Journal*, V. 49, No. 1, January–February, pp. 92–103.
16. Naaman, A. E. and Alkhairi, F. M., 1991, "Stress at Ultimate in Unbonded Post-Tensioning Tendons: Part 2-Proposed Methodology," *ACI Structural Journal*, V. 88, No. 6, November–December, pp. 683–692.
17. ACI Committee 318, 2002, *Building Code Requirements for Structural Concrete* (318-02) *and Commentary* (318R-02), American Concrete Institute, Farmington Hills, MI, 443 pp.
18. Grace, N. F., 2000, "Transfer Lengths of CFRP/CFCC Strands for DT-Girders," *PCI Journal*, V. 45, No. 5, September–October, pp. 110–126.
19. Zou, P. X. W., 2003, "Long-Term Properties and Transfer Length of Fiber Reinforced Polymers," *Journal of Composites for Construction*, ASCE, V. 7, No. 1, pp. 10–19.
20. British Standards Institution, 1995, "Structural Use of Concrete: Code of Practice for Design and Construction," BS 8110: Part 1-1985, London.